Article

Adverse Crosstalk Between Extracellular Matrix Remodeling and Ferroptosis in Basal Breast Cancer

Christophe Desterke [1,*], Emma Cosialls [2,3], Yao Xiang [2], Rima Elhage [2,3], Clémence Duruel [2,3], Yunhua Chang [2] and Ahmed Hamaï [2,3,*]

[1] UFR Médecine-INSERM UMS33, Université Paris-Sud, F94800 Villejuif, France ; christophe.desterke@inserm.fr (C.D.)

[2] Université Paris Cité, INSERM UMR-S1151, CNRS UMR-S8253, Institut Necker Enfants Malades, and [3] Team 5/Ferostem group, F-75015 Paris, France ; emma.cosialls@inserm.fr (E.C.) ; xiangyao.ecole@outlook.com (Y.X.) ; rima.elhage@inserm.fr (R.E.) ; clemence.duruel@inserm.fr (C.D.) ; yunhua.chang-marchand@inserm.fr (Y.C.) ; ahmed.hamai@inserm.fr (A.H.)

* Correspondence: christophe.desterke@inserm.fr (C.D.); ahmed.hamai@inserm.fr (A.H.)

Abstract: (1) Background: Breast cancer is a frequent heterogeneous disorder diagnosed in woman and is a high cause of mortality of them in reason to rapid metastasis and disease recurrence. Ferroptosis can inhibit breast cancer cell growth, improve the sensitivity of chemotherapy and radiotherapy and inhibit distant metastases so potentially acts on tumor micro-environment; (2) Methods: Ferroptosis/Extracellular matrix remodeling literature text-mining results were integrated in breast cancer transcriptome cohort according their distant relapse free survival (DRFS) under adjuvant therapy (anthracyclin+taxanes) and also in MDA-MB-231 transcriptome functional experiments with ferroptosis activations (GSE173905); (3) Results: Ferroptosis/Extracellular matrix remodeling text-mining identified 910 associated genes in at list 10 articles. Univariate Cox analyses censored on breast cancer (GSE25066) selected 252 individual significant genes and 171 of them found with an adverse expression. Functional enrichment of these 171 adverse genes predicted basal breast cancer signatures. By text-mining some ferroptosis significant adverse selected genes shared citations in domain of ECM remodeling such as: TNF, IL6, SET, CDKN2A, EGFR, HMGB1, KRAS, MET, LCN2, HIF1A, TLR4. A molecular score based on expression the eleven genes was found predictive of worst prognosis breast cancer at univariate level: basal subtype, short DRFS, high grade values 3 and 4, estrogen and progesterone receptors negative and nodal stages 2 and 3. This eleven gene signature was validated as regulated by ferroptosis inductors (erastin and RSL3) in triple negative breast cancer cellular model MDA-MB-231.; (4) Conclusions: Crosstalk between ECM remodeling-Ferroptosis functionalities allowed to define a molecular score which have been characterized as an independent adverse parameter in prognosis of breast cancer patients. Gene signature of this molecular score have been validated to be regulated by erastin/RSL3 ferroptosis activators. This molecular score could be promising to evaluate ECM impact of ferroptosis target therapies in breast cancer.

Keywords: basal breast cancer; extracellular matrix remodeling; ferroptosis; transcriptome; text mining

1. Introduction

The breast cancer is the most common cancer newly diagnosed for women in United States in 2020 [1]. Breast cancer is a heterogeneous disease with different molecular subtypes defined by distinct molecular classes associated to prognosis: claudin-low, normal-like, luminal A, luminal B, HER2

 doi:10.20944/preprints202306.0642.v1

and basal [2] and confirmed by gene quantification in pam50 classification [3]. Breast cancer is the second leading cause of mortality in woman due to rapid metastasis and disease recurrence [4]. The breast tissue is in a unique microenvironment with plentiful adipocytes infiltrating. Previous studies have shown that adipocytes can regulate fatty acid metabolism, enhance the invasion and metastasis of breast cancer [5]. Ferroptosis is an iron-dependent regulated form of cell death caused by the accumulation of lipid-based reactive oxygen species (ROS) [6]. Prerequisites for ferroptosis include iron metabolism, mitochondrial metabolism, synthesis of polyunsaturated fatty acid phospholipid (PUFA-PL) and lipid peroxidation [7]. Targeting ferroptosis have been proposed to treat breast cancer. There is increasing evidence that ferroptosis can inhibit breast cancer cell growth, improve the sensitivity of chemotherapy and radiotherapy and inhibit distant metastases [5]. From 2001 to 2003, the Stockwell Lab performed a screen to identify compounds that kill cells engineered to be tumourigenic (harbouring the RAS mutant), without killing their isogenic parental precursors. One of the most efficient compounds was identified and named "erastin" after its ability to "Eradicate RAS-and Small T transformed cells" [8]. Subsequently, they identified RSL3, which was also named after its "oncogenic-RAS-selective lethal" property in 2008 [9]. Small molecule–induced ferroptosis has been shown to have a strong inhibitory effect on tumor growth in a drug-resistant environment, which may increase the sensitivity of the tumor to chemotherapeutic treatment [10]. Ferroptosis is also considered an important cell death mechanism caused by a number of therapies, including chemotherapy, radiotherapy (RT), targeted therapy and immunotherapy [11], but in opposite way, the tumor cells with ferroptosis could diminish anti-tumor immune response by inhibiting the antigen presenting cells [12]. The tumor microenvironment (TME) plays a notable role in cancer progression. It includes pH and oxygen levels, the extracellular matrix (ECM), connective tissue, infiltrating immune cells, and the vasculature of the tumor. Interaction between the ECM and the tumor cells activates key signaling pathways that promote tumor proliferation, invasion, and metastasis. This notably influences many tumors as the ECM can comprise up to 60% of the tumor mass [13].

In the present work, by a text-mining approach integrated in transcriptome experiments, a link between Ferroptosis and ECM remodeling was done through gene related regulation in adverse prognosis of breast cancer but also in TNBC cellular model stimulated by ferroptosis activators.

2. Materials and Methods

Determination of ferroptosis in breast related genes

Using keyword "Ferroptosis in breast" keyword, a co-occurrence of citations with coding gene identifiers was searched in the article abstracts of the PUBMED database was searched with the "Génie" algorithm [14]. Bioinformatics analyses were realized in R software environment version 4.2.1. False Discovery Rate (FDR) of the significant associated genes were analyzed by qqplot visualization with qqman R package version 0.1.8 [15]. Further investigations of text-mining associations with gene identifiers have been confirmed with the "GeneValorization" application [16] on the National Center for Biotechnolgy Information (NCBI) database [17]. The results of this text-mining were drawn as circleplot of gene-keywords co-occurrence with circlize R-package version 0.4.15 and as alluvial plot.

Transcriptome cohort of breast cancer for patients treated with anthracyclin and taxanes

Transcriptome normalized matrix of dataset GSE25066 [18] was downloaded at the following address: https://www.ncbi.nlm.nih.gov/geo/query/acc.cgi?acc=gse25066 (accessed on 2023, may 18th) and annotated with the corresponding technology platform GPL96 [HG-U133A] Affymetrix Human Genome U133A Array available at the following address: https://www.ncbi.nlm.nih.gov/geo/query/acc.cgi?acc=GPL96 (accessed on 2023, may 18th).

Transcriptome dataset testing effect of ferroptosis activators on MDA-MB-231 triple negative breast cancer cell line

 doi:10.20944/preprints202306.0642.v1

Fragments Per Kilobase of transcript sequence per Millions base pairs sequenced (FPKM) Transcript quantification performed by original pipeline of dataset GSE173905 [19] were downloaded at the following address:https://www.ncbi.nlm.nih.gov/geo/query/acc.cgi?acc=GSE173905 (accessed on 2023, may 18th). After sequencing on Illumina NovaSeq 6000 technology, the original pipeline aligned reads on human genome with the reference genome was built using Hisat2 v2.0.5 [20] and paired-end clean reads were aligned to the reference genome using Hisat2 v2.0.5 software and FPKM, expected number of Fragments Per Kilobase of transcript sequence per Millions base pairs sequenced were computed on counts obtained with Feature Counts v1.5.0-p3 software [21]. On selected genes for Ferroptosis/Extracellular matrix remodeling signature, unsupervised principal component analysis was performed with FactoMiner R package version 2.8 [22].

Gene expression analyses and association to the breast cancer prognosis

Distant relapse free survival (DRFS) from dataset GSE25066 [18] was used as outcome to performed iterative univariate Cox analysis against expression of the genes identified as being significantly associated with the keyword "ferroptosis in breast". During trial follow-up of adjuvant therapy in breast cancer, distant relapse–free survival (DRFS) could be used as endpoint [18]. DRFS was defined as the interval from initial diagnostic biopsy until diagnosis of distant metastasis or death from breast cancer, non-breast cancer, or unknown causes [23]. This iteration of univariate Cox analysis was automatized with loopcolcox R-package version 1.0.0 available at the following address: https://github.com/cdesterke/loopcolcox (accessed on 2023, may 18th). Univariate Kaplan Meier and survival optimal threshold on variables were performed with survminer R-package version 0.4.9 and survival R-package version 3.3.1. On genes with adverse prognosis association a functional enrichment was performed with CPG signature from MsigDb database [24] through Toppgene online application [25]. A breast cancer related signature network was drawn with Cytoscape standalone software version 3.9.1 [26]. An expression molecular score related to Ferroptosis/Extracellular matrix remodeling functionalities was done by computing the sum of the product between Cox beta coefficients and expression of the eleven selected genes. For the eleven genes belonging to the Ferroptosis/Extracellular matrix remodeling signature a multi-ROC analysis was done against estrogen/progesterone receptors status detected in immunohistochemistry with the R-package multirocauc version 1.0.0 available at the address: https://github.com/cdesterke/multirocauc (accessed on 2023, may 18th) (**Supplemental Figure 1A**). A multivariate Cox model was built with DRFS as outcome and with incorporation of molecular score and relevant clinical parameters. This DRFS multivariate model was assessed by testing linearity of residuals at global level and for each individual included parameters with Schoenfeld tests. Calibration of the DRFS multivariate model at 10 months of follow-up was done by 500 iterations of bootstrap with rms R-package version 6.7.0. Nomogram validated at 10 months of follow-up was drawn for DRFS multivariate model with regplot R-package version 1.1.

3. Results

3.1. Ferroptosis gene expression associated to the prognosis of patients with breast cancer

A text-mining approach was employed to found genes related to the ferroptosis in breast literature. The text-mining algorithm “Génie” was employed by querying Pubmed with “ferroptosis in breast” keywords. This query returns a list of 910 individual genes with significant False Discovery Rate (FDR) and positive in at least 10 distinct articles (**Figure 1A**). Iterations of univariate Cox analyses against distant relapse free survival (DRFS) outcome of patients from transcriptome dataset GSE25066 [18] was done for each of the 910 genes selected by text-mining. For best fifty ranked genes associated in their expression to the prognosis of the patients, some of them were found favorable and other adverse according the sense of their beta coefficients or hazard ratios (**Figure 1B**). For example, PTTG1 (PTTG1 regulator of sister chromatid separation, securin) is the ferroptosis in breast related gene found with the most adverse expression in breast cancer samples (hazard ratio=2.21)

Preprints (www.preprints.org) | NOT PEER-REVIEWED | Posted: 8 June 2023 doi:10.20944/preprints202306.0642.v1

followed by ENO1 (enolase 1) with hazard ratio 2.23, SLC7A5 (solute carrier family 7 member 5) with hazard ratio 1.51, ITCH (itchy E3 ubiquitin protein ligase) with hazard ratio 3.86, EGLN1 (egl-9 family hypoxia inducible factor 1) with hazard ratio 2.26 (**Figure 1B** and **Supplemental Table 1**).

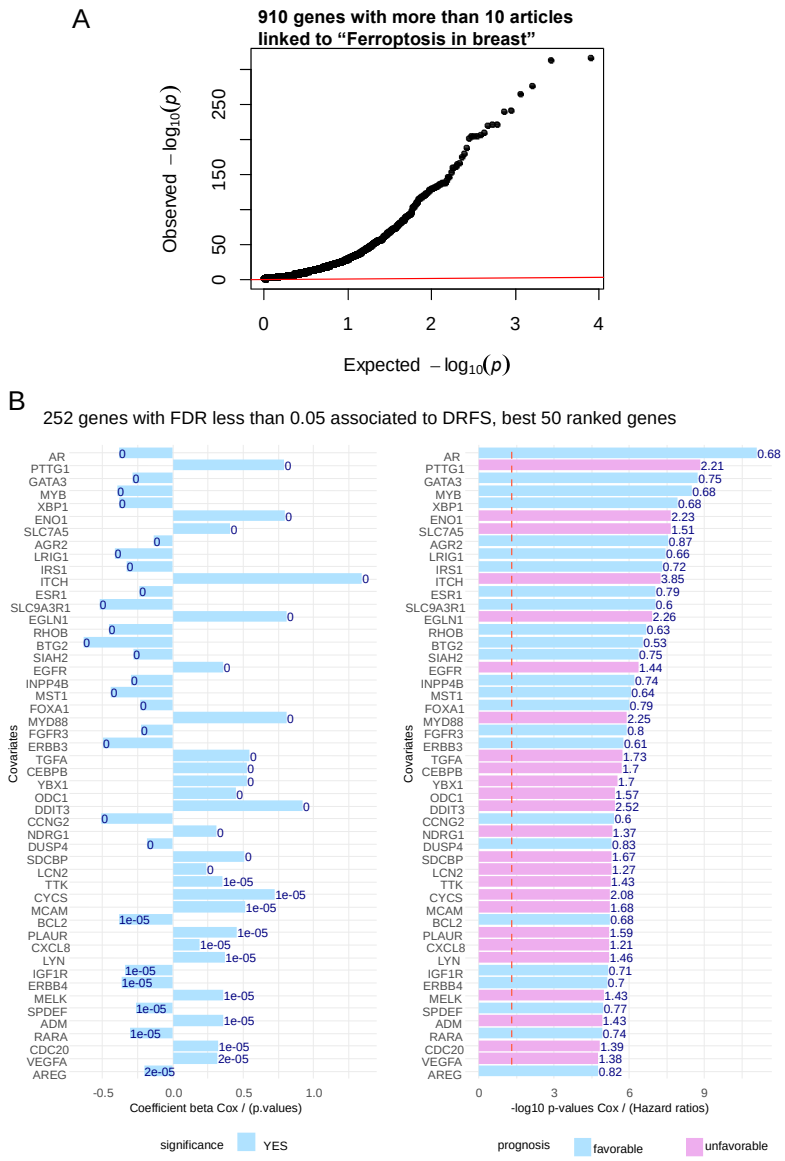

Figure 1. Gene expression profile related to ferroptosis functionality is associated to disease free relapse survival in breast cancer: A/ Qqplot of the False Discovery Rate (FDR) q-values from genes related to ferroptosis in breast; B/ Barplots of univariate Cox beta coefficients and negative log10 p-values for the 50 best ferroptosis related genes according Disease Free Relapse Survival (DFRS) of breast cancer patients (transcriptome GSE25066, n=508).

Among the 252 significant genes associated to the prognosis, a filtration on positivity of Cox beta-coefficients was done to retain 171 genes associated to adverse prognosis. Functional enrichment performed with these 171 adverse genes on MsigDb CPG signature database highlighted main enrichment with of these genes in breast cancer published signatures such as: SMID-breast cancer basal up [27] and SOTIRIOU-breast cancer grade 1 vs 3 up [28] (**Figure 2A**). A breast cancer network was drawn with the ferroptosis. Some ferroptosis-related genes were found shared between the two independent breast cancer transcriptome cohort signatures (**Figure 2B**), such as: FOXM1 (forkhead box M1), SLC7A5 (solute carrier family 7 member 5), CHEK1 (checkpoint kinase 1), MKI67 (marker of

 doi:10.20944/preprints202306.0642.v1

proliferation Ki-67), TTK (TTK protein kinase), PTTG1 (PTTG1 regulator of sister chromatid separation), BIRC5 (baculoviral IAP repeat containing 5), MELK (maternal embryonic leucine zipper kinase), CCNA2 (cyclin A2), NEK2 (NIMA related kinase 2), TPX2 (TPX2 microtubule nucleation factor), CDK1 (cyclin dependent kinase 1) and CDC20 (cell division cycle 20). These results suggest that the ferroptosis in breast related text-mining approach allowed to predict breast cancer transcriptome experiments already published and among these genes some are associated to adverse prognosis of the patients. To validate Génie text-mining approach an independent text-mining algorithm "GeneValorization" was employed still to query PUBMED database with "ferroptosis" keyword but also some others with relevance in the context of the study such as: cancer stem cell (CSC), Extracellular matrix (ECM) remodeling, breast cancer, lipid peroxidation and regulated cell death. This validation allowed to highlight best 15 top ranked genes in text-mining sharing these keywords associations (**Figure 2C**): SET (S (ET nuclear proto-oncogene), TNF (tumor necrosis factor), HMOX1 (heme oxygenase 1), IL6 (interleukin 6), TRFC (transferrin receptor), ATF4 (activating transcription factor 4), HMGB1 (high mobility group box 1), KRAS (KRAS proto-oncogene, GTPase), EGFR (epidermal growth factor receptor), TLR4 (toll like receptor 4), HIF1A (hypoxia inducible factor 1 subunit alpha), ATG5 (autophagy-related 5), LCN2 (lipocalin 2), CDKN2A (cyclin dependent kinase inhibitor 2A), MET (MET proto-oncogene, receptor tyrosine kinase).

Preprints (www.preprints.org) | NOT PEER-REVIEWED | Posted: 8 June 2023 doi:10.20944/preprints202306.0642.v1

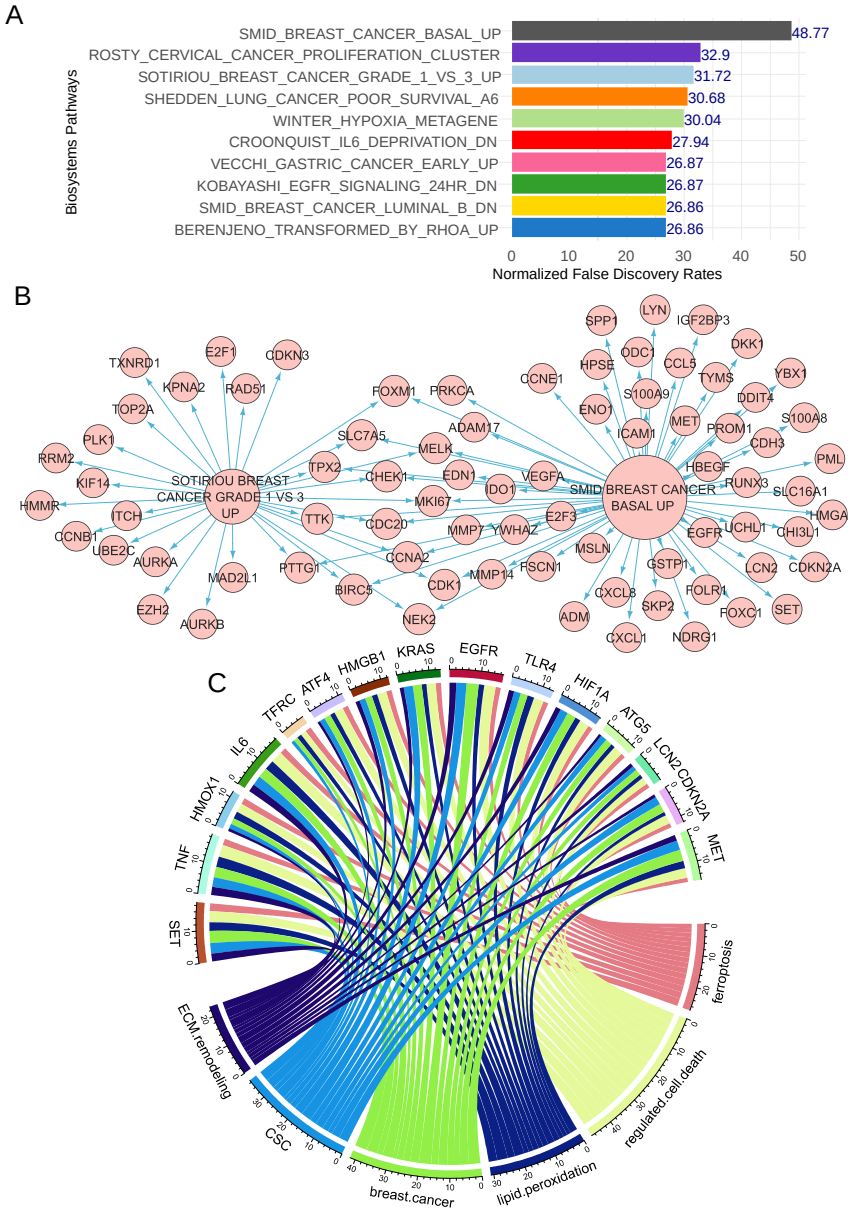

Figure 2. Unfavorable ferroptosis related genes were found enriched in basal breast cancer: A/ Barplot of functional enrichment performed on "MSIGDB CPG" database with the 170 unfavorable ferroptosis genes; B/ Functional enrichment network of 170 unfavorable ferroptosis genes enriched on advanced breast cancer signatures; C/ Circosplot of 15 best ferroptosis genes most cited in literature associated to keywords: extracellular matrix (ECM) remodeling, cancer stem cell (CSC), breast cancer, lipid peroxidation, regulated cell death and ferroptosis.

3.2. Ferroptosis/extracellular matrix remodeling expression score and prognosis in breast cancer

Among ferroptosis validated genes in breast cancer (**Figure 2C**), eleven of them harbored some association with extracellular matrix remodeling literature in PUBMED database, especially: TNF, SET and IL6 were found highly cited in this specific literature (**Figure 3A**). Exploring individual expression of these eleven genes against immunohistochemistry status of estrogen receptor highlighted great importance of expression for CDKN2A (aera under curve (AUC: 0.76) and EGFR (AUC: 0.79) (**Figure 3B**) for this hormonal prediction. Unsupervised principal component analysis based on expression of the eleven ferroptosis/extracellular matrix remodeling-related genes well stratified patient groups according their estrogen receptor status on first principal axis (**Supplemental Figure**

Preprints (www.preprints.org) | NOT PEER-REVIEWED | Posted: 8 June 2023 doi:10.20944/preprints202306.0642.v1

2A). Concerning immunohistochemistry status of progesterone receptor, expression of CDKN2A appeared decisive (AUC: 0.72, **Figure 3C**).

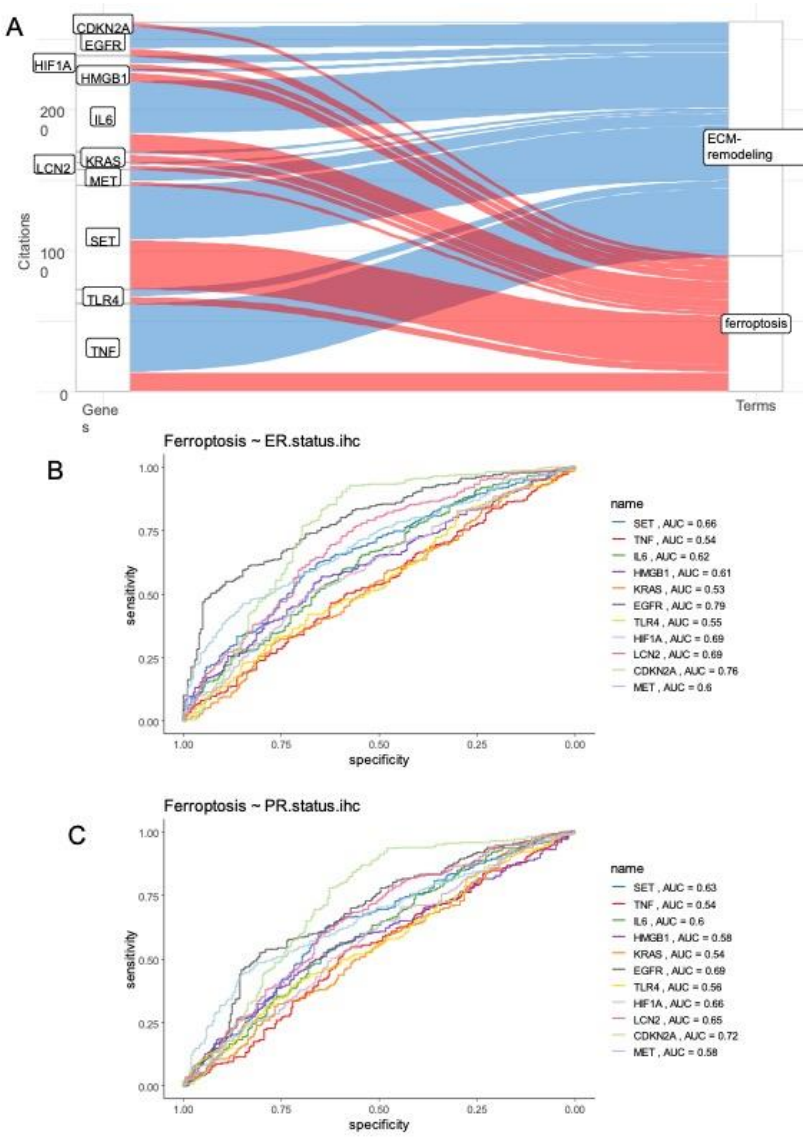

Figure 3. Eleven gene signature shared between ferroptosis and extracellular matrix remodeling functionalities: A/ Alluvial plot of literature citation counts for best 11 genes with co-occurence in ferroptosis and extracellular matrix remodeling (ECM) functionalities; B/ Multi-ROC analysis of expression (GSE25066) for the 11 genes against estrogen receptor detection; C/ Multi-ROC analysis of expression (GSE25066) for the 11 genes against progesterone receptor detection.

Unsupervised principal component analysis based on expression of the eleven ferroptosis/extracellular matrix remodeling-related genes well stratified groups of patients according their progesterone receptor status on first principal axis (**Supplemental Figure 2B**). Similarly, principal component analysis gradually stratified tumor grades on the first principal axis (**Figure 4A**), and pam50 molecular groups (**Figure 4B**) suggesting that the eleven gene signature related to ferroptosis/ECM remodeling could be interesting for prognostication of the breast cancer patients. A molecular score was computed on the expression of the eleven ferroptosis/extracellular matrix remodeling related genes. Optimal cutpoint was determined on DRFS residuals of the molecular score (**Figure 4C**). This threshold cutpoint was found at 48.74 to stratify the breast cancer cohort in two groups. No significant

Preprints (www.preprints.org) | NOT PEER-REVIEWED | Posted: 8 June 2023 doi:10.20944/preprints202306.0642.v1

difference was found between the two groups of patients harboring low and high values of ferroptosis/ECM remodeling molecular score (p-value=0.52, **Table 1**). Concerning immunohistochemistry status of estrogen receptor, a significant higher proportion of negative patients was found in group of patients with high values of molecular score (p-value<1E-4, **Table 1**), and it was the same observation for progesterone receptor status (p-value<1E-4, **Table 1**). Concerning pam50 molecular classification, groups of patients with high values of ferroptosis/ECM remodeling score present higher proportion of basal type samples (p-value<1E-4, **Table 1**). No significant difference was observed on tumor stages between the two groups of patients (p-value=0.38, **Table 1**) but a higher proportion of patients N3 for nodal status was observed in group of patients with high value of molecular score (p-value=0.013, **Table 1**). Concerning clinical AJCC staging a significant difference was observed with increase proportion of stages IIIA, IIIB, IIIC and inflammatory in group of patients with high value of molecular score (p-value=0.03, **Table 1**). As observed by PCA on the expression of the eleven genes which composed the molecular score (**Figure 4A**), the grade variable was found significant between the two groups of patients (p-value<1E-4, **Table 1**). DRFS status and time parameters were also confirmed as significant between the two groups of patients (p-value<1E-4, **Table 1**). Effectively, Kaplan Meier with DRFS censor stratified on ferroptosis/ECM remodeling is very significant (**Figure 4D**), with a major worst prognosis for patients which harbored a molecular score over 48.74 as threshold. Type of taxanes (Taxol, Taxotere) administrated during follow-up of the patients present no associations with the Ferroptosis/ECM remodeling groups of patients (p-value=0.69, **Table 1**).

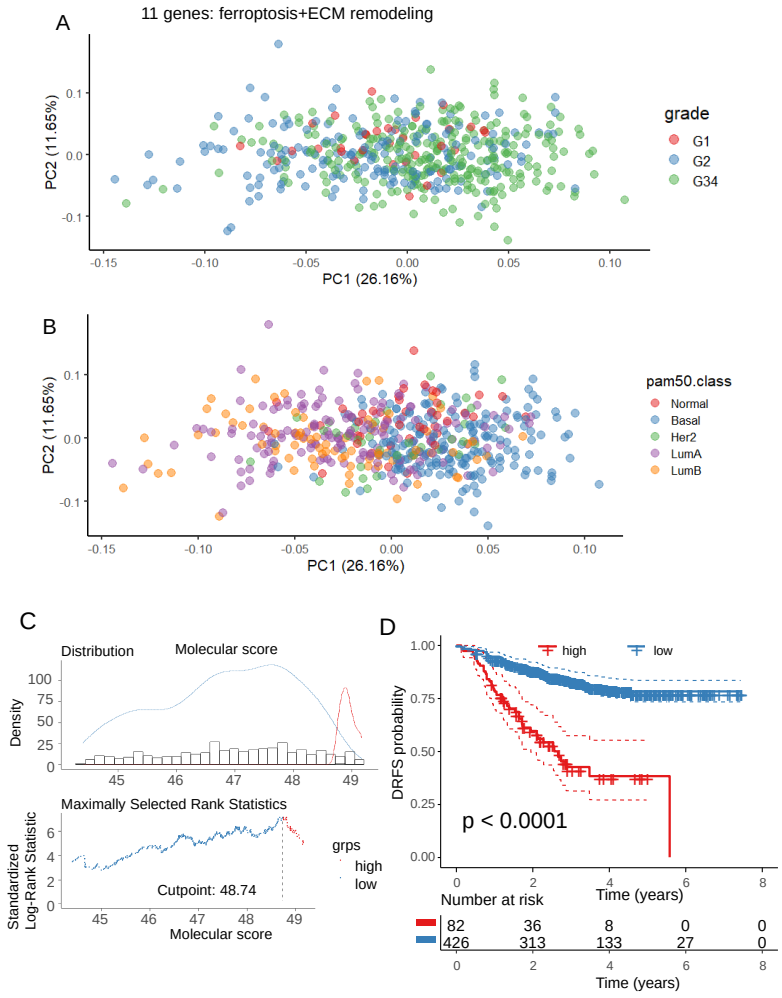

Figure 4. Ferroptosis/Extracellular matrix remodeling molecular score is associated to the worst therapy response in breast cancer: Unsupervised principal component analysis performed with eleven gene signature and stratified : A/ On grade of the tumors (grades 3 and 4 were aggregated in one

Preprints (www.preprints.org) | NOT PEER-REVIEWED | Posted: 8 June 2023 doi:10.20944/preprints202306.0642.v1

class), B/ On pam50 molecular classification of breast tumors, C/ Optimal threshold cutpoint determined for ferroptosis/ECM remodeling molecular score censored on DRFS(distant relapse free survival); D/ Kaplan Meier and log rank analyses censored on DRFS and stratified on ferroptosis/ECM remodeling molecular score threshold.

Table 1. Breast cancer cohort from dataset GSE25066 stratified according high and low levels of Ferroptosis/Extracellular matrix remodeling molecular score.

Variable	Level	low (n=426)	high (n= 82)	Total (n=508)	p-value
age.years	mean (sd)	49.7 (10.4)	50.5 (10.8)	49.8 (10.5)	0.524161
age.categories (40.3 yo)	younger	79 (18.5)	20 (24.4)	99 (19.5)	
	older	347 (81.5)	62 (75.6)	409 (80.5)	0.283927
er.status.ihc	Negative	144 (34.1)	61 (76.2)	205 (40.8)	
	Positive	278 (65.9)	19 (23.8)	297 (59.2)	< 1e-04
	missing	4	2	6	
pr.status.ihc	Negative	192 (45.6)	66 (82.5)	258 (51.5)	
	Positive	229 (54.4)	14 (17.5)	243 (48.5)	< 1e-04
	missing	5	2	7	
pam50.class	Normal	42 (9.9)	2 (2.4)	44 (8.7)	
	Basal	123 (28.9)	66 (80.5)	189 (37.2)	
	Her2	33 (7.7)	4 (4.9)	37 (7.3)	
	LumA	152 (35.7)	8 (9.8)	160 (31.5)	
	LumB	76 (17.8)	2 (2.4)	78 (15.4)	< 1e-04
clinical.tumor.stage	T-0,1,2	247 (58.0)	41 (50.0)	288 (56.7)	
	T-3	119 (27.9)	26 (31.7)	145 (28.5)	
	T-4	60 (14.1)	15 (18.3)	75 (14.8)	0.379010
clinical.nodal.status	N-0	140 (32.9)	17 (20.7)	157 (30.9)	
	N-1	205 (48.1)	39 (47.6)	244 (48.0)	
	N-2,3	81 (19.0)	26 (31.7)	107 (21.1)	0.013986
clinical.ajcc.stage	IIB	131 (30.8)	20 (24.4)	151 (29.7)	
	IIIA	99 (23.2)	22 (26.8)	121 (23.8)	
	IIIB	63 (14.8)	17 (20.7)	80 (15.7)	
	IIA	109 (25.6)	12 (14.6)	121 (23.8)	
	IIIC	16 (3.8)	7 (8.5)	23 (4.5)	
	Inflammatory	2 (0.5)	2 (2.4)	4 (0.8)	
	I	6 (1.4)	2 (2.4)	8 (1.6)	0.033976
grade	G-1	32 (7.8)	0 (0.0)	32 (6.6)	
	G-2	167 (40.8)	13 (16.9)	180 (37.0)	
	G-3,4	210 (51.3)	64 (83.1)	274 (56.4)	< 1e-04
	missing	17	5	22	
drfs.status	1	70 (16.4)	41 (50.0)	111 (21.9)	
	0	356 (83.6)	41 (50.0)	397 (78.1)	< 1e-04
drfs.time.years	mean (sd)	3.2 (1.6)	2 (1.2)	3 (1.6)	< 1e-04
type.taxane	Taxotere	78 (45.6)	14 (51.9)	92 (46.5)	
	Taxol	93 (54.4)	13 (48.1)	106 (53.5)	0.691854
	missing	255	55	310	

Relevant clinical parameters were integrated in a multivariable Cox model censored on DRFS with group stratification based on ferroptosis/ECM remodeling molecular score. This multivariable model which harbored a concordant index of 0.77 was found highly significant by likelihood ratio test (p-value=2E-14) (**Figure 5A**). Global and individual Schoenfeld test attested linear distribution residuals from included parameters: age of patients, nodal status, pam50 molecular classification, grading, and ferroptosis/ECM remodeling molecular score (**Supplemental Figure 3**). In this multivariable model high values of nodal status (N1 and N2,3) were found as independent adverse parameter of DRFS (N1 versus N0 hazard ratio: 2.20, p-value=5.91E-3, N23 versus N0 hazard ratio: 3.39, p-value=7.15E-5, **Table 2** and **Figure 5A**). Among molecular classification, basal subtype appeared as adverse group of breast cancer with normal like as reference (Hazard ratio:2.92, p-value 4.45E-2, **Table 2** and **Figure 5A**). In the DRFS multivariate model, ferroptosis/ECM remodeling molecular score

Preprints (www.preprints.org) | NOT PEER-REVIEWED | Posted: 8 June 2023 doi:10.20944/preprints202306.0642.v1

appeared as an adverse independent parameter in the prognosis of breast cancer patients (high score vs low score hazard ratio: 2.69, p-value=1.17E-5). The multivariate model could be calibrated at ten months of follow-up with five hundred iterations by Kaplan Meier method (**Figure 5B**): this calibration showed that the multivariable model is stable at 10 months of follow-up because near of ideal model in gray. The corresponding nomogram of the model was drawn for a prediction at 10 months of follow up (**Figure 5C**). This representation confirms the important part of the molecular score in the multivariate model. Indeed, at 10 months of follow-up, the molecular score appears dispersed between the range of point values of the model (10-70) for a DRFS probability at 10 months comprised between (0.006 and 0.1) (**Figure 5C**).

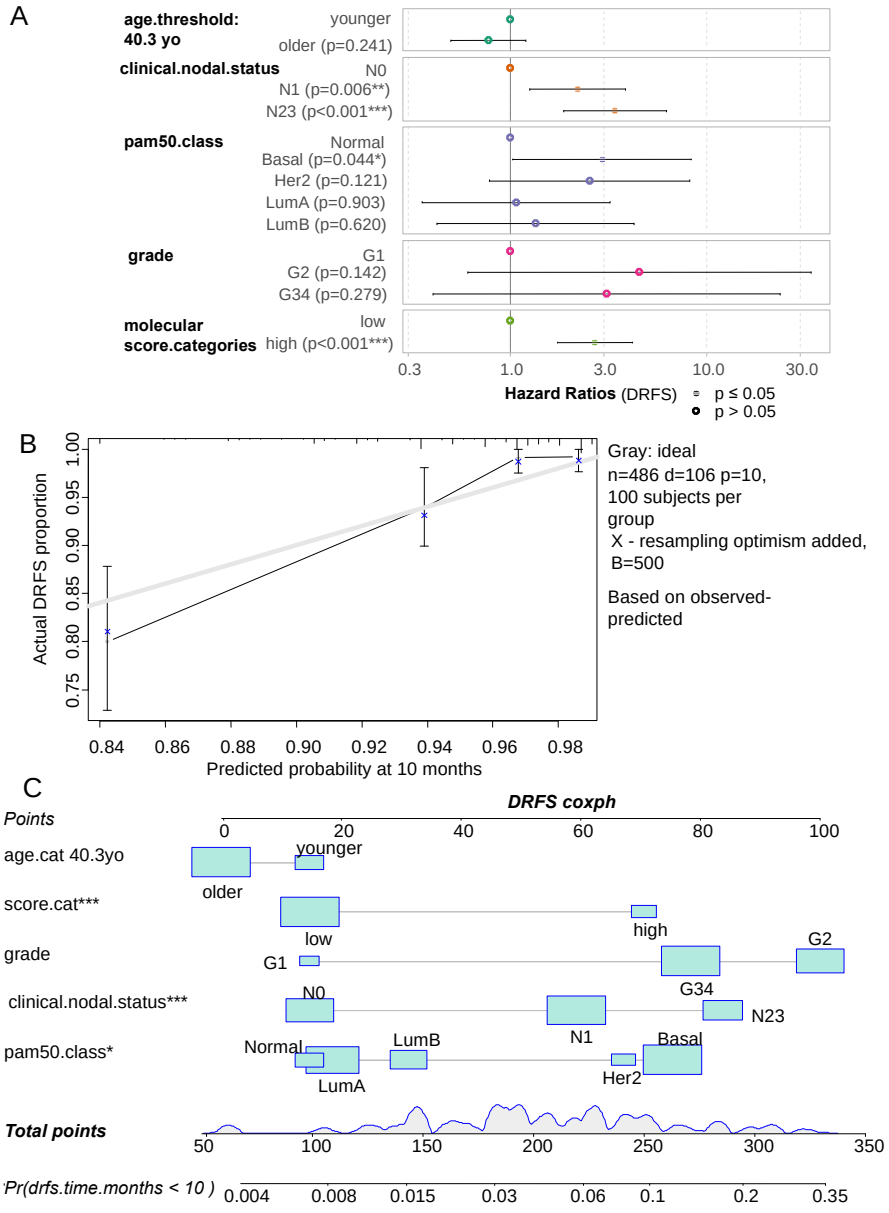

Figure 5. Ferroptosis/Extracellular matrix remodeling molecular score is an independent adverse parameter in prognosis of breast cancer patients: A/ Forestplot of multivariable model censored on distant relapse free survival and including ferroptosis/Extracellular matrix remodeling and clinico-biological relevant parameters such as: age nodular status, grade and molecule classes.; B/ Bootstrap calibration plot of the DRFS multivariable model performed with 500 iterations with Kaplan Meier method at 10 months of follow; C/ Nomogram of the DRFS multivariable model predict at 10 months of follow.

 doi:10.20944/preprints202306.0642.v1

Table 2. Disease free relapse survival multivariate model including Ferroptosis/Extracellular matrix remodeling molecular score.

variables	Hazard ratios	Confidence-low	Confidence-high	P-value
age.cat older	0.770	0.498	1.192	2.41E-01
clinical.nodal.statusN1	2.202	1.255	3.862	5.91E-03
clinical.nodal.statusN23	3.395	1.857	6.205	7.15E-05
pam50.classBasal	2.924	1.027	8.327	4.45E-02
pam50.classHer2	2.530	0.783	8.177	1.21E-01
pam50.classLumA	1.071	0.356	3.221	9.03E-01
pam50.classLumB	1.339	0.422	4.252	6.20E-01
Grade.G2	4.526	0.603	33.950	1.42E-01
Grade.G34	3.085	0.402	23.693	2.79E-01
score.high	2.689	1.728	4.185	1.17E-05

3.3. Ferroptosis/ECM remodeling signature is regulated by ferroptosis activators in triple negative breast cancer cells

To verify ferroptosis functional of gene members belonging to the molecular score, transcriptome of MDA-MB-231 cells (cellular model of Triple Negative Breast Cancer (TNBC)) stimulated by two distinct ferroptosis activators: erastin and RSL3 was analyzed (GSE173905) [19]. Based on the expression of the eleven genes belonging to ferroptosis/ECM molecular score, an unsupervised principal component analysis was performed with samples of GSE173905. This multivariate analysis confirmed that gene members composing the molecular score are regulated by the two distinct ferroptosis activators: erastin and RSL3 (p-value=1.08E-5, **Figure 6A**). During this ferroptosis functional activations, gene members are regulated by distinct patterns (**Figure 6B**). Some genes like HIF1A (**Figure 6C**) and LCN2, EGFR, IL6 (**Figure 6D**) were found up regulated by both ferroptosis activators. Some genes like HMGB1, KRAS, SET (**Figure 6E**) were found down regulated by both ferroptosis activators. MET and TLR4 were found regulated in opposite way by the two ferroptosis activators (**Figure 6F**). Finally, TNF and CDKN2A were not found detected by sequencing in this MDA-MB-231 TNBC cellular model.

Preprints (www.preprints.org) | NOT PEER-REVIEWED | Posted: 8 June 2023 doi:10.20944/preprints202306.0642.v1

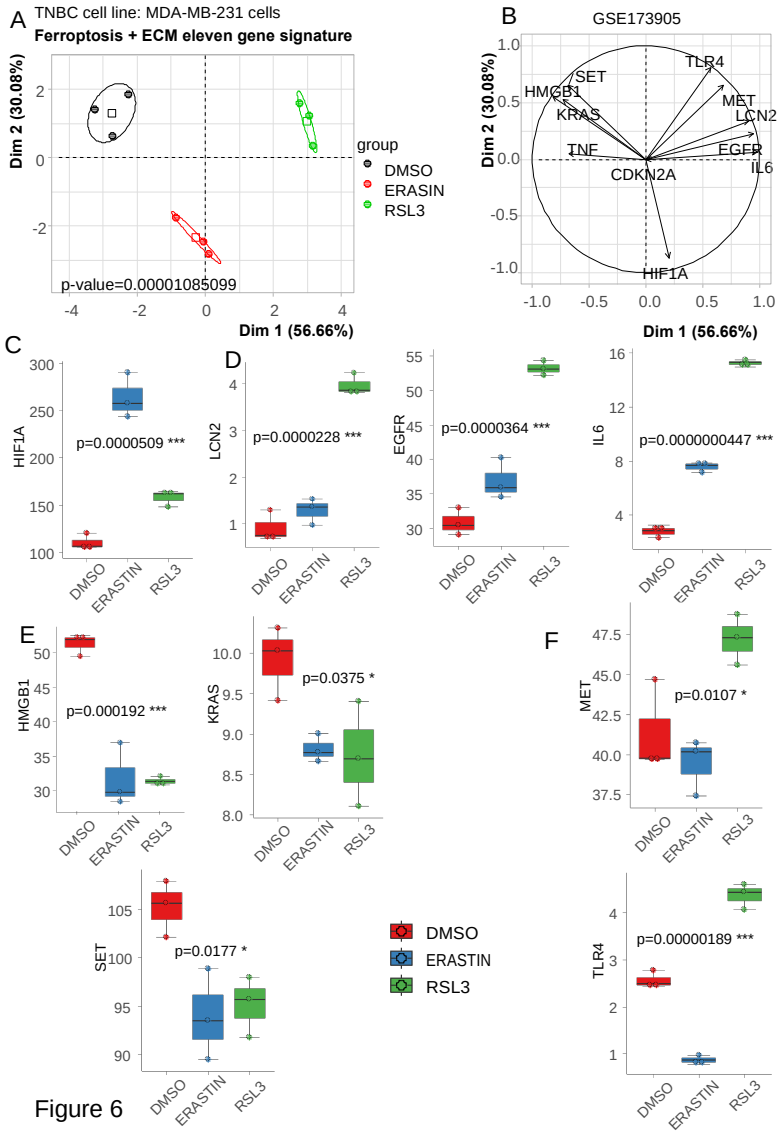

Figure 6

Figure 6. Regulation of the Ferroptosis/Extracellular matrix remodeling signature by ferroptosis activators in triple negative breast cancer cellular model: A/ First principal map representative of 86 percent of regulation for the ferroptosis/Extracellular matrix remodeling markers; B/ Principal component correlation plot of the expression for ferroptosis/Extracellular matrix remodeling markers analyzed in MDA-MB-231 cells stimulated by erastin and RSL3 ferroptosis activators; C/ Up regulation of HIF1A by both ferroptosis activators; D/ Up regulation of LCN2, EGFR, IL6 by both ferroptosis activators; E/ Down regulation of HMGB1, KRAS, SET by both ferroptosis activators; F/ Inverted regulation of MET, TLR4 by the distinct ferroptosis activators.

4. Discussion

During this study, by text mining approach, a list of genes was defined as related to ferroptosis cellular functionality known as important way cellular death implicated in tumor response to therapies [10]. Surprisingly, in transcriptome of breast tumors under therapies (GSE173905) [18], the majority of ferroptosis-related genes were found having expression associated with adverse distant relapse free survival: 171 of 252 significant genes were found with univariate hazard ratio over 1 (**Supplemental Table 1**). With an independent text mining application querying NCBI database: GeneValorization [16], it could be able to establish a Ferroptosis/ECM remodeling molecular score in basal breast cancer [18] based on the expression of eleven related genes: TNF, IL6, SET, CDKN2A, EGFR, HMGB1, KRAS, MET, LCN2, HIF1A, TLR4. Except CDKN2A and TNF, the majority of these

 doi:10.20944/preprints202306.0642.v1

implicated genes have been validated as been expressed in TNBC cellular model MDA-MB-231 and regulated by ferroptosis activators: erastin and RSL3 [8,9].

HIF-1α is an important regulator of the lipid metabolism [29]. Hypoxia-induced lipid metabolism reprogramming results in fatty acid accumulation, which promotes tumor growth and survival upon reoxidation [30]. Ferroptosis induction with erastin or RSL3 showed a significant up regulation of HIF1A in TNBC cell line. In the context of increased hypoxia/HIF1A and ECM stiffness in chemoresistant tumors, high expression of HIF1A could be adverse because its is leading to upregulation of ITGA5, activation of the downstream FAK/Src signaling pathways and repression of miR-326 which targets fibronectin (FN1), an extracellular matrix (ECM) central chemoresistance driver gene [31]. The adipokine Lipocalin-2 (LCN2) has been demonstrated to be an ECM regulator through its association with the ECM protease matrix metalloproteinase-9 (MMP-9) [32]. It has been shown that LCN2 knockout in human breast cancer cell line MDA-MB-231 ameliorates erastin-mediated ferroptosis and increases cisplatin vulnerability [33].

Adipocytes constitute the main cell component of ECM in breast cancer [34]. Cancer-associated adipocytes (CAAs) are localized at the invasive front of breast tumor and exhibit a modified phenotype, a loss of lipid content, a decrease in late adipocyte differentiation markers and overexpression of inflammatory cytokines and proteases [35]. IL6 up regulation was promoted by ferroptosis activators in MDA-MB-231 TNBC cellular model (**Figure 6D**). In breast tumors, IL6 is secreted by CAAs which play essential roles in favor of proliferation, angiogenesis, dissemination, invasion and metastasis of breast cancer [36]. In breast cancer, the pleiotropic cytokine IL-6 production is related to the development of stem cell phenotype, angiogenesis, cachexia, and resistance to therapy [37].

EGFR overexpression was found under ferroptosis stimulation in MDA-MB-231 cells (**Figure 6D**). EGFR promoted TNBC cell clustering and blockade of EGFR successfully abolished tumor cell cluster formation [38]. It has been shown that inhibition of EGFR signaling pathway significantly suppressed cell viability of TNBC cells and reduced fraction of CSCs with intracellular enhancement of lipid peroxidation when TNBC cells exposed to erastin [39].

MET is known to be implicated in chemotherapy resistance especially resistance to targeted therapies, including those targeting EGFR, BRAF and MEK but also contributes to cytotoxic chemotherapy resistance [40]. Its ligand, HGF is a pleiotropic factor produced by mesenchymal cells in the stroma and as such is widely distributed in the extracellular matrix of most tissues [41]. Dysregulation of the MET/HGF pathway leads to uncontrolled cell proliferation and oncogenesis and is observed in multiple tumour types [42]. There is few link between MET and ferroptosis except that HGF exacerbated pancreatic cancer cell ferroptosis resistance [43]. In the present work, it was observed that RSL3 ferroptosis activator induced overexpression of MET in MDA-MB-231 TNBC cellular model.

In MDA-MB-231, it was observed a significant down regulation of High-mobility group box 1 (HMGB1). HMGB1 control chromosomal structure and is considered as a redox-sensitive protein. HMGB1 is implicated in regulating stress responses to oxidative damage and cell death, which are closely related to the pathology of inflammatory diseases such as cancer. HMGB1 can also be released into the extracellular space and function as a damage-associated molecular pattern protein during ferroptosis [44]. HMGB1 is known to act via the NRF2/GPX4 axis to repress ferroptosis in mesangial cells in response to high glucose [45].

In ER-positive breast cancer, SET overexpression reduced tamoxifen-induced antitumor effects and may contribute to the failure of the tamoxifen treatment by modulating the ER signaling [46]. In MDA-MB-231 TNBC cellular model, ferroptosis activation shown a major repression of SET proto-oncogene.

Ferroptosis activators induced repression of KRAS oncogene expression in MDA-MB-231 TNBC cellular model. KRAS mutations are known as very infrequent in triple-negative breast tumors [47], but in basal breast cancer, KRAS have been shown to promote the mesenchymal features of this aggressive cancer [48].

Overexpression of Toll-like receptor-4 (TLR4) in human tumors often correlates with chemoresistance and metastasis. Depletion of TLR4 in naturally overexpressing MDA-MB-231 cells

 doi:10.20944/preprints202306.0642.v1

downregulated prosurvival genes concomitant with 2- to 3-fold reduced IC(50) to paclitaxel in vitro and a 6-fold decrease in recurrence rate in vivo [49]. Effect of ferroptosis activators Erastin and RSL3 on MDA-MB-231 showed an opposite effect on TLR4 expression.

In the present work, by a text mining approach integrated in distinct transcriptome dataset, we could elucidate an adverse molecular program which crosstalk between ferroptosis and extracellular remodeling functionalities during basal breast cancer. This adverse regulated program allowed to compute a molecular expression score that could be promising to evaluate response of ferroptosis target therapies in breast cancer.

Supplementary Materials: The following supporting information can be downloaded at: www.mdpi.com/xxx/s1, Figure S1 related to Figure 1: Progesterone and estrogen receptors status of ferroptosis/ECM remodeling gene signature; Figure S2 related to Figure 3: Age influence on distant relapse free survival in breast cancer; Figure S3 related to Figure 5: Global and individual Schoenfeld tests for the multivariate distant relapse free survival model and their included parameters; Table S1: t List of the univariate Cox analysis for the 252 ferroptosis related significant genes against Distant Free Relapse Survival in transcriptome cohort (GSE25066).

Author Contributions: CC and AH conceptualized, interpreted the data, and wrote the manuscript. EC, YX, RE, CD and YC provided a critical review of the data and manuscript. All authors have read and agreed to the published version of the manuscript.".

Funding: This work was supported by core funding from University, CNRS and INSERM. AH was supported by grants from Comité de Paris de la ligue contre le cancer.

Acknowledgments: The authors gratefully acknowledge funding from INSERM, Université Paris Cité, la ligue nationale contre le cancer, and Comité de Paris de la ligue contre le cancer.

Conflicts of Interest: The authors declare no conflict of interest.

References

1. Siegel, R.L.; Miller, K.D.; Jemal, A. Cancer Statistics, 2020. *CA A Cancer J Clin* **2020**, *70*, 7–30, doi:10.3322/caac.21590.
2. Perou, C.M.; Sørlie, T.; Eisen, M.B.; van de Rijn, M.; Jeffrey, S.S.; Rees, C.A.; Pollack, J.R.; Ross, D.T.; Johnsen, H.; Akslen, L.A.; et al. Molecular Portraits of Human Breast Tumours. *Nature* **2000**, *406*, 747–752, doi:10.1038/35021093.
3. Bastien, R.R.L.; Rodríguez-Lescure, Á.; Ebbert, M.T.W.; Prat, A.; Munárriz, B.; Rowe, L.; Miller, P.; Ruiz-Borrego, M.; Anderson, D.; Lyons, B.; et al. PAM50 Breast Cancer Subtyping by RT-QPCR and Concordance with Standard Clinical Molecular Markers. *BMC Med Genomics* **2012**, *5*, 44, doi:10.1186/1755-8794-5-44.
4. Subhan, M.A.; Parveen, F.; Shah, H.; Yalamarty, S.S.K.; Ataide, J.A.; Torchilin, V.P. Recent Advances with Precision Medicine Treatment for Breast Cancer Including Triple-Negative Sub-Type. *Cancers (Basel)* **2023**, *15*, 2204, doi:10.3390/cancers15082204.
5. Liu, Y.; Hu, Y.; Jiang, Y.; Bu, J.; Gu, X. Targeting Ferroptosis, the Achilles' Heel of Breast Cancer: A Review. *Front Pharmacol* **2022**, *13*, 1036140, doi:10.3389/fphar.2022.1036140.
6. Dixon, S.J.; Lemberg, K.M.; Lamprecht, M.R.; Skouta, R.; Zaitsev, E.M.; Gleason, C.E.; Patel, D.N.; Bauer, A.J.; Cantley, A.M.; Yang, W.S.; et al. Ferroptosis: An Iron-Dependent Form of Nonapoptotic Cell Death. *Cell* **2012**, *149*, 1060–1072, doi:10.1016/j.cell.2012.03.042.
7. Tang, D.; Kroemer, G. Ferroptosis. *Current Biology* **2020**, *30*, R1292–R1297, doi:10.1016/j.cub.2020.09.068.
8. Dolma, S.; Lessnick, S.L.; Hahn, W.C.; Stockwell, B.R. Identification of Genotype-Selective Antitumor Agents Using Synthetic Lethal Chemical Screening in Engineered Human Tumor Cells. *Cancer Cell* **2003**, *3*, 285–296, doi:10.1016/S1535-6108(03)00050-3.
9. Yang, W.S.; Stockwell, B.R. Synthetic Lethal Screening Identifies Compounds Activating Iron-Dependent, Nonapoptotic Cell Death in Oncogenic-RAS-Harboring Cancer Cells. *Chemistry & Biology* **2008**, *15*, 234–245, doi:10.1016/j.chembiol.2008.02.010.

10. Luis, G.; Godfroid, A.; Nishiumi, S.; Cimino, J.; Blacher, S.; Maquoi, E.; Wery, C.; Collignon, A.; Longuespée, R.; Montero-Ruiz, L.; et al. Tumor Resistance to Ferroptosis Driven by Stearoyl-CoA Desaturase-1 (SCD1) in Cancer Cells and Fatty Acid Biding Protein-4 (FABP4) in Tumor Microenvironment Promote Tumor Recurrence. *Redox Biology* **2021**, *43*, 102006, doi:10.1016/j.redox.2021.102006.
11. Hassannia, B.; Vandenabeele, P.; Vanden Berghe, T. Targeting Ferroptosis to Iron Out Cancer. *Cancer Cell* **2019**, *35*, 830–849, doi:10.1016/j.ccell.2019.04.002.
12. Sacco, A.; Battaglia, A.M.; Botta, C.; Aversa, I.; Mancuso, S.; Costanzo, F.; Biamonte, F. Iron Metabolism in the Tumor Microenvironment—Implications for Anti-Cancer Immune Response. *Cells* **2021**, *10*, 303, doi:10.3390/cells10020303.
13. Henke, E.; Nandigama, R.; Ergün, S. Extracellular Matrix in the Tumor Microenvironment and Its Impact on Cancer Therapy. *Front. Mol. Biosci.* **2020**, *6*, 160, doi:10.3389/fmolb.2019.00160.
14. Fontaine, J.-F.; Priller, F.; Barbosa-Silva, A.; Andrade-Navarro, M.A. Génie: Literature-Based Gene Prioritization at Multi Genomic Scale. *Nucleic Acids Res.* **2011**, *39*, W455-461, doi:10.1093/nar/gkr246.
15. D. Turner, S. Qqman: An R Package for Visualizing GWAS Results Using Q-Q and Manhattan Plots. *JOSS* **2018**, *3*, 731, doi:10.21105/joss.00731.
16. Brancotte, B.; Biton, A.; Bernard-Pierrot, I.; Radvanyi, F.; Reyal, F.; Cohen-Boulakia, S. Gene List Significance At-a-Glance with GeneValorization. *Bioinformatics* **2011**, *27*, 1187–1189, doi:10.1093/bioinformatics/btr073.
17. Sayers, E.W.; Barrett, T.; Benson, D.A.; Bryant, S.H.; Canese, K.; Chetvernin, V.; Church, D.M.; DiCuccio, M.; Edgar, R.; Federhen, S.; et al. Database Resources of the National Center for Biotechnology Information. *Nucleic Acids Res.* **2009**, *37*, D5-15, doi:10.1093/nar/gkn741.
18. Hatzis, C. A Genomic Predictor of Response and Survival Following Taxane-Anthracycline Chemotherapy for Invasive Breast Cancer. *JAMA* **2011**, *305*, 1873, doi:10.1001/jama.2011.593.
19. Li, P.; Lin, Q.; Sun, S.; Yang, N.; Xia, Y.; Cao, S.; Zhang, W.; Li, Q.; Guo, H.; Zhu, M.; et al. Inhibition of Cannabinoid Receptor Type 1 Sensitizes Triple-Negative Breast Cancer Cells to Ferroptosis via Regulating Fatty Acid Metabolism. *Cell Death Dis* **2022**, *13*, 808, doi:10.1038/s41419-022-05242-5.
20. Kim, D.; Langmead, B.; Salzberg, S.L. HISAT: A Fast Spliced Aligner with Low Memory Requirements. *Nat Methods* **2015**, *12*, 357–360, doi:10.1038/nmeth.3317.
21. Liao, Y.; Smyth, G.K.; Shi, W. FeatureCounts: An Efficient General Purpose Program for Assigning Sequence Reads to Genomic Features. *Bioinformatics* **2014**, *30*, 923–930, doi:10.1093/bioinformatics/btt656.
22. Lê, S.; Josse, J.; Husson, F. FactoMineR: An R Package for Multivariate Analysis. *Journal of Statistical Software* **2008**, *25*, 1–18.
23. Hudis, C.A.; Barlow, W.E.; Costantino, J.P.; Gray, R.J.; Pritchard, K.I.; Chapman, J.-A.W.; Sparano, J.A.; Hunsberger, S.; Enos, R.A.; Gelber, R.D.; et al. Proposal for Standardized Definitions for Efficacy End Points in Adjuvant Breast Cancer Trials: The STEEP System. *JCO* **2007**, *25*, 2127–2132, doi:10.1200/JCO.2006.10.3523.
24. Liberzon, A.; Birger, C.; Thorvaldsdóttir, H.; Ghandi, M.; Mesirov, J.P.; Tamayo, P. The Molecular Signatures Database (MSigDB) Hallmark Gene Set Collection. *Cell Syst* **2015**, *1*, 417–425, doi:10.1016/j.cels.2015.12.004.
25. Chen, J.; Bardes, E.E.; Aronow, B.J.; Jegga, A.G. ToppGene Suite for Gene List Enrichment Analysis and Candidate Gene Prioritization. *Nucleic Acids Res.* **2009**, *37*, W305-311, doi:10.1093/nar/gkp427.
26. Cline, M.S.; Smoot, M.; Cerami, E.; Kuchinsky, A.; Landys, N.; Workman, C.; Christmas, R.; Avila-Campilo, I.; Creech, M.; Gross, B.; et al. Integration of Biological Networks and Gene Expression Data Using Cytoscape. *Nat Protoc* **2007**, *2*, 2366–2382, doi:10.1038/nprot.2007.324.

27. Smid, M.; Wang, Y.; Zhang, Y.; Sieuwerts, A.M.; Yu, J.; Klijn, J.G.M.; Foekens, J.A.; Martens, J.W.M. Subtypes of Breast Cancer Show Preferential Site of Relapse. *Cancer Research* **2008**, *68*, 3108–3114, doi:10.1158/0008-5472.CAN-07-5644.
28. Sotiriou, C.; Neo, S.-Y.; McShane, L.M.; Korn, E.L.; Long, P.M.; Jazaeri, A.; Martiat, P.; Fox, S.B.; Harris, A.L.; Liu, E.T. Breast Cancer Classification and Prognosis Based on Gene Expression Profiles from a Population-Based Study. *Proc Natl Acad Sci U S A* **2003**, *100*, 10393–10398, doi:10.1073/pnas.1732912100.
29. Shen, G.-M.; Zhao, Y.-Z.; Chen, M.-T.; Zhang, F.-L.; Liu, X.-L.; Wang, Y.; Liu, C.-Z.; Yu, J.; Zhang, J.-W. Hypoxia-Inducible Factor-1 (HIF-1) Promotes LDL and VLDL Uptake through Inducing VLDLR under Hypoxia. *Biochemical Journal* **2012**, *441*, 675–683, doi:10.1042/BJ20111377.
30. Bensaad, K.; Favaro, E.; Lewis, C.A.; Peck, B.; Lord, S.; Collins, J.M.; Pinnick, K.E.; Wigfield, S.; Buffa, F.M.; Li, J.-L.; et al. Fatty Acid Uptake and Lipid Storage Induced by HIF-1α Contribute to Cell Growth and Survival after Hypoxia-Reoxygenation. *Cell Reports* **2014**, *9*, 349–365, doi:10.1016/j.celrep.2014.08.056.
31. Assidicky, R.; Tokat, U.M.; Tarman, I.O.; Saatci, O.; Ersan, P.G.; Raza, U.; Ogul, H.; Riazalhosseini, Y.; Can, T.; Sahin, O. Targeting HIF1-Alpha/MiR-326/ITGA5 Axis Potentiates Chemotherapy Response in Triple-Negative Breast Cancer. *Breast Cancer Res Treat* **2022**, *193*, 331–348, doi:10.1007/s10549-022-06569-5.
32. Rebalka, I.A.; Monaco, C.M.F.; Varah, N.E.; Berger, T.; D'souza, D.M.; Zhou, S.; Mak, T.W.; Hawke, T.J. Loss of the Adipokine Lipocalin-2 Impairs Satellite Cell Activation and Skeletal Muscle Regeneration. *Am J Physiol Cell Physiol* **2018**, *315*, C714–C721, doi:10.1152/ajpcell.00195.2017.
33. Valashedi, M.R.; Roushandeh, A.M.; Tomita, K.; Kuwahara, Y.; Pourmohammadi-Bejarpasi, Z.; Kozani, P.S.; Sato, T.; Roudkenar, M.H. CRISPR/Cas9-Mediated Knockout of Lcn2 in Human Breast Cancer Cell Line MDA-MB-231 Ameliorates Erastin-Mediated Ferroptosis and Increases Cisplatin Vulnerability. *Life Sci* **2022**, *304*, 120704, doi:10.1016/j.lfs.2022.120704.
34. Lee, Y.; Jung, W.H.; Koo, J.S. Adipocytes Can Induce Epithelial-Mesenchymal Transition in Breast Cancer Cells. *Breast Cancer Res Treat* **2015**, *153*, 323–335, doi:10.1007/s10549-015-3550-9.
35. Dirat, B.; Bochet, L.; Dabek, M.; Daviaud, D.; Dauvillier, S.; Majed, B.; Wang, Y.Y.; Meulle, A.; Salles, B.; Le Gonidec, S.; et al. Cancer-Associated Adipocytes Exhibit an Activated Phenotype and Contribute to Breast Cancer Invasion. *Cancer Res* **2011**, *71*, 2455–2465, doi:10.1158/0008-5472.CAN-10-3323.
36. Zhao, C.; Wu, M.; Zeng, N.; Xiong, M.; Hu, W.; Lv, W.; Yi, Y.; Zhang, Q.; Wu, Y. Cancer-Associated Adipocytes: Emerging Supporters in Breast Cancer. *J Exp Clin Cancer Res* **2020**, *39*, 156, doi:10.1186/s13046-020-01666-z.
37. Gyamfi, J.; Eom, M.; Koo, J.-S.; Choi, J. Multifaceted Roles of Interleukin-6 in Adipocyte-Breast Cancer Cell Interaction. *Transl Oncol* **2018**, *11*, 275–285, doi:10.1016/j.tranon.2017.12.009.
38. Liu, X.; Adorno-Cruz, V.; Chang, Y.-F.; Jia, Y.; Kawaguchi, M.; Dashzeveg, N.K.; Taftaf, R.; Ramos, E.K.; Schuster, E.J.; El-Shennawy, L.; et al. EGFR Inhibition Blocks Cancer Stem Cell Clustering and Lung Metastasis of Triple Negative Breast Cancer. *Theranostics* **2021**, *11*, 6632–6643, doi:10.7150/thno.57706.
39. Wu, X.; Sheng, H.; Zhao, L.; Jiang, M.; Lou, H.; Miao, Y.; Cheng, N.; Zhang, W.; Ding, D.; Li, W. Co-Loaded Lapatinib/PAB by Ferritin Nanoparticles Eliminated ECM-Detached Cluster Cells via Modulating EGFR in Triple-Negative Breast Cancer. *Cell Death Dis* **2022**, *13*, 557, doi:10.1038/s41419-022-05007-0.
40. Wood, G.E.; Hockings, H.; Hilton, D.M.; Kermorgant, S. The Role of MET in Chemotherapy Resistance. *Oncogene* **2021**, *40*, 1927–1941, doi:10.1038/s41388-020-01577-5.
41. Matsumoto, K.; Nakamura, T. Roles of HGF as a Pleiotropic Factor in Organ Regeneration. *EXS* **1993**, *65*, 225–249.
42. Tovar, E.A.; Graveel, C.R. MET in Human Cancer: Germline and Somatic Mutations. *Ann. Transl. Med.* **2017**, *5*, 205–205, doi:10.21037/atm.2017.03.64.

43. Wu, Q.; Song, L.; Guo, Y.; Liu, S.; Wang, W.; Liu, H.; Gong, A.; Liao, X.; Zhu, H.; Wang, D. Activated Stellate Cell Paracrine HGF Exacerbated Pancreatic Cancer Cell Ferroptosis Resistance. *Oxid Med Cell Longev* **2022**, *2022*, 2985249, doi:10.1155/2022/2985249.
44. Chen, R.; Zou, J.; Kang, R.; Tang, D. The Redox Protein High-Mobility Group Box 1 in Cell Death and Cancer. *Antioxid Redox Signal* **2023**, doi:10.1089/ars.2023.0236.
45. Wu, Y.; Zhao, Y.; Yang, H.-Z.; Wang, Y.-J.; Chen, Y. HMGB1 Regulates Ferroptosis through Nrf2 Pathway in Mesangial Cells in Response to High Glucose. *Biosci Rep* **2021**, *41*, BSR20202924, doi:10.1042/BSR20202924.
46. Huang, Y.-H.; Chu, P.-Y.; Chen, J.-L.; Huang, C.-T.; Lee, C.-H.; Lau, K.-Y.; Wang, W.-L.; Wang, Y.-L.; Lien, P.-J.; Tseng, L.-M.; et al. SET Overexpression Is Associated with Worse Recurrence-Free Survival in Patients with Primary Breast Cancer Receiving Adjuvant Tamoxifen Treatment. *J Clin Med* **2018**, *7*, 245, doi:10.3390/jcm7090245.
47. Sánchez-Muñoz, A.; Gallego, E.; de Luque, V.; Pérez-Rivas, L.G.; Vicioso, L.; Ribelles, N.; Lozano, J.; Alba, E. Lack of Evidence for KRAS Oncogenic Mutations in Triple-Negative Breast Cancer. *BMC Cancer* **2010**, *10*, 136, doi:10.1186/1471-2407-10-136.
48. Kim, R.-K.; Suh, Y.; Yoo, K.-C.; Cui, Y.-H.; Kim, H.; Kim, M.-J.; Gyu Kim, I.; Lee, S.-J. Activation of KRAS Promotes the Mesenchymal Features of Basal-Type Breast Cancer. *Exp Mol Med* **2015**, *47*, e137, doi:10.1038/emm.2014.99.
49. Rajput, S.; Volk-Draper, L.D.; Ran, S. TLR4 Is a Novel Determinant of the Response to Paclitaxel in Breast Cancer. *Mol Cancer Ther* **2013**, *12*, 1676–1687, doi:10.1158/1535-7163.MCT-12-1019.